Difficulties in determining electrical anisotropy in subsurface investigations[1]

Niels B. Christensen[2]

Abstract

Surface electrical and electromagnetic methods have a limited resolution capability for determining the conductivity structure of the earth. In one-dimensional modelling a collection of many thin layers is frequently considered as one composite layer, which is then macro-anisotropic. Neither galvanic methods nor inductive methods alone can resolve the anisotropy of the ground, but a joint inversion of galvanic and inductive data may do so. The necessity of including the coefficient of anisotropy in the joint inversion of galvanic and inductive sounding data is demonstrated. An analysis is made of the combined use of geoelectrical and transient soundings to resolve the coefficient of anisotropy of a subsurface layer for varying thickness, resistivity and coefficient of anisotropy. It is found that the coefficient of anisotropy is well resolved only for layers that are many times thicker than the overburden and for coefficients of anisotropy that are not too small. The ability of the joint inversion of geoelectrical and transient sounding data to resolve macro-anisotropic layers is tested using realistic earth models determined from electrical logs.

Introduction

The concepts of homogeneity and isotropy play an important role in electromagnetic modelling. Usually we consider models to be composed of elements that are homogeneous and isotropic, whether the models be one-, two- or three-dimensional. However, real geological formations may exhibit anisotropy in two ways. Firstly, the formation may be intrinsically anisotropic because of the microstructure of the formation. In this category we find clays that, due to the elongated shape of the individual mineral grains and the processes of deposition, can have a better conductivity in the direction parallel to the grain planes. Secondly, surface electrical and electromagnetic methods can achieve only limited resolution of the conductivity structure of the subsurface, and in 1D modelling we often have to consider a collection of many thin layers as one composite layer, which is then macro-anisotropic. Macro-anisotropy is also found in cases of a fractured subsurface (Campbell 1977). In this study of 1D modelling, it is assumed that the conductivity is the same in all horizontal

---

directions, but is different in the vertical direction, i.e. a transversely isotropic layered model.

Neither galvanic methods nor inductive methods alone can resolve the anisotropy of the ground. However, a joint inversion of galvanic and inductive data requires that anisotropy be taken into account and it can also resolve the coefficient of anisotropy, thus contributing to a more detailed description of the subsurface resistivity structure (Jupp and Vozoff 1977).

The determination of electrical anisotropy is desirable as it may indicate the presence of otherwise unresolved thin layers. From a hydrogeological point of view, these may severely influence the hydraulic flow pattern in the ground. Thin clay layers in an otherwise sandy formation will lower the vertical hydraulic conductivity considerably and will deflect infiltration, and thin sand and gravel layers in an otherwise clayey formation may serve as fast hydraulic conduction channels for polluted water. In the mapping of raw materials, anisotropy indicates that the material under investigation is not homogeneous throughout and may thus be of inferior quality (Christensen 1992).

In the following, an analysis of the importance of taking anisotropy into account in inverse modelling is presented, and it is shown how the combined use of geoelectrical and transient soundings can resolve the coefficient of anisotropy of a subsurface layer.

Anisotropy, scale and resolution

Whether or not the concepts of homogeneity and isotropy are valid approximations to the complexities of the real world is a matter of dimension, i.e. the scale on which the subsurface is modelled. On a scale of the size of individual mineral grains, a formation is obviously not homogeneous and isotropic. On a somewhat larger scale, the grain structure becomes unimportant but anisotropy may arise from the microfacies of the formation. On a larger scale involving tens of metres, we may see thin layers, for example clay and silt in a sand formation. If we model the earth with a layer spanning such a depth interval, the sand formation taken as a whole will exhibit macro-anisotropy.

In a parametric 1D inversion of data from electrical and electromagnetic surface methods, the subsurface is modelled with as few layers as possible to satisfy the data and the *a priori* knowledge of the geology. Due to the limited resolution capabilities of electrical and electromagnetic methods, these model layers often consist of many thinner real layers and the effective layer resistivities and thicknesses of the model layers are generally different from those of their composite real layers. These model layers can be described by considering them as macro-anisotropic layers, for which electrical fields can be modelled (Sinha and Bhattacharya 1967; Chlamtac and Abramovici 1981).

The coefficient of anisotropy of a homogeneous transversely isotropic layer is defined by

$$\lambda = \sqrt{\rho_v/\rho_h}, \tag{1}$$
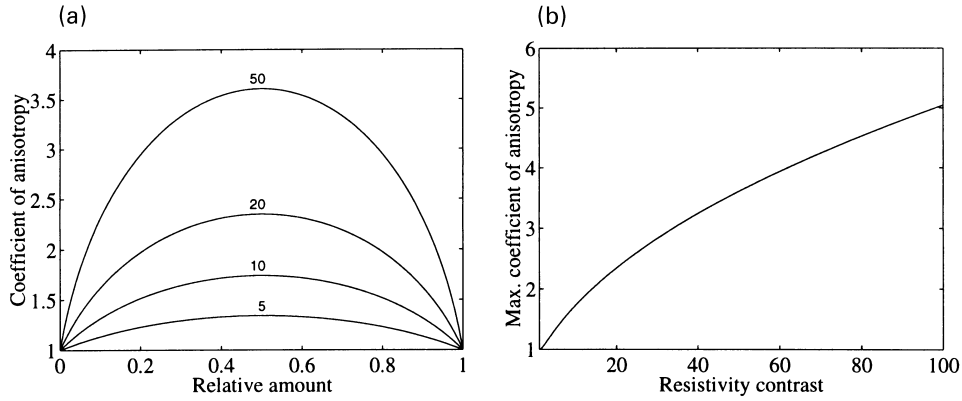
Figure 1. (a) A plot of the coefficient of anisotropy as a function of the relative amount of one formation in a layer consisting of two formations for different resistivity contrasts $\beta = 5, 10, 20, 50$. (b) The maximum coefficient of anisotropy for a two-component layer plotted as a function of the resistivity contrast.

where ρ_v is the resistivity in the vertical direction and ρ_h is the resistivity in the horizontal direction (Keller and Frischknecht 1966).

For a sequence of m layers with resistivities ρ_i and thicknesses h_i, we find

$$\rho_v = T/H, \quad \rho_h = H/S, \quad \lambda = \sqrt{\rho_v/\rho_h} = \sqrt{ST/H^2}, \tag{2}$$

where

$$T = \sum_{i=1}^{m} \rho_i h_i, \quad S = \sum_{i=1}^{m} h_i/\rho_i \quad \text{and} \quad H = \sum_{i=1}^{m} h_i. \tag{3}$$

T denotes the vertical resistance, S denotes the horizontal conductance and H denotes the total thickness of the sequence.

In the special case, where only two different resistivities are present, we can express the coefficient of anisotropy of the interbedded section in terms of α, the accumulated thickness of medium 1 relative to the total thickness, and β, the resistivity contrast defined as the quotient of the resistivities of medium 1 and medium 2. Using the above formulae we find

$$\lambda = \sqrt{\alpha^2 + (1 - \alpha)^2 + \alpha(1 - \alpha)(\beta + 1/\beta)}. \tag{4}$$

As expected the formula is symmetric in α and $(1 - \alpha)$ and also in β and $1/\beta$. In Fig. 1a, the coefficient of anisotropy, λ, is shown as a function of α for different β.

The maximum coefficient of anisotropy, obtainable with two media present, is reached when they appear in equal amounts ($\alpha = 1/2$). In this case we find

$$\lambda_{max} = \frac{1 + \beta}{2\sqrt{\beta}} \Leftrightarrow \beta = [\lambda + \sqrt{\lambda^2 - 1}]^2. \tag{5}$$

If we have determined a certain coefficient of anisotropy of a macro-anisotropic layer, the minimum resistivity contrast between two media that could have produced the observed anisotropy can be found from (5). In Fig. 1b, the maximum coefficient of anisotropy, λ_{max}, is shown as a function of β.

Anisotropy and joint inversion

Let us consider the two fundamental methods of current conduction in the ground: galvanic electrical methods (DC or direct current geoelectrical methods), where current is injected into the ground by means of grounded electrodes, and inductive electromagnetic methods, where current is induced in the ground by means of a primary magnetic field changing with time.

The geoelectrical sounding method is based on galvanic conduction of current in the ground and has for a long time been one of the most popular and frequently used geophysical electrical methods. The interpretation of data from geoelectrical soundings using a 1D plane parallel earth model has shown that the electrical anisotropy of the layers cannot be resolved. An anisotropic layer is equivalent to an isotropic layer of thickness h_{GAL}, equal to the product of the coefficient of anisotropy and the true thickness, and of resistivity ρ_{GAL}, equal to the mean resistivity (Keller and Frischknecht 1966), so that

$$h_{\mathrm{GAL}} = \lambda \cdot h \qquad \text{and} \qquad \rho_{\mathrm{GAL}} = \lambda \cdot \rho_{\mathrm{h}} = \sqrt{\rho_{\mathrm{v}} \cdot \rho_{\mathrm{h}}} = \rho_{\mathrm{m}}. \qquad (6)$$

Not only is the coefficient of anisotropy undetermined, but we see that the interpretation is compromised by the presence of anisotropic layers. For coefficients of anisotropy that are not too high, the error in the determination of the layer resistivities will usually result in a correct geological interpretation of the physical model, since different geological units often have a greater difference in resistivity than the error introduced from anisotropy. However, the distortion of layer thicknesses is more severe, especially in connection with quantitative estimates of depths and volumes. It is a fact that the thickness of a layer is never better determined than the coefficient of anisotropy. This is most often (conveniently?) forgotten in connection with geoelectrical soundings.

It is irrelevant to include the coefficient of anisotropy in the description of the model. We have no way of detecting this parameter, since it does not reveal itself in the measurements in a way that distinguishes the data set from that of a 1D isotropic model.

Inductive methods will only determine the horizontal resistivity of a layer, while the thickness is undistorted, so that

$$h_{\mathrm{IND}} = h \quad \text{and} \quad \rho_{\mathrm{IND}} = \rho_{\mathrm{h}}. \qquad (7)$$

Time-domain and frequency-domain electromagnetic methods in the quasi-static approximation with sources on or above a horizontally stratified ground will only give rise to horizontal current flow in the ground, and so only the horizontal resistivity of the

ground is of importance in this case. The layer thicknesses determined are not affected by the presence of anisotropy, and the conductivity of a composite anisotropic layer is equal to the mean horizontal conductivity of the actual depth interval.

That the current flow in a stratified ground is only horizontal is evident in the case of a vertical magnetic dipole source, but is somewhat counter-intuitive in the case of a horizontal magnetic dipole source. For the horizontal magnetic dipole source, Ward and Hohmann (1989) give the formula for the galvanic Schelkunoff potential (p. 224, equation (4.109)), from which it is seen that the galvanic Schelkunoff potential on or above the surface vanishes in the quasi-static approximation. Since it is the solution of a second-order differential equation, the galvanic Schelkunoff potential must be zero everywhere below the surface where no source discontinuities occur and thus there will be no vertical electric field component.

In the remainder of this paper the term 'inductive methods' is taken to mean 'inductive methods in the quasi-static approximation'.

In the case of electromagnetic inductive methods, as for galvanic methods, we see that it is irrelevant to include the coefficient of anisotropy in the model, since it does not influence the data. It is only the horizontal resistivity which is important.

Thus neither galvanic methods nor inductive methods used alone will resolve the coefficients of anisotropy. However, as suggested by the above formulae, a joint inversion of data from galvanic and inductive methods may determine the coefficient of anisotropy (Jupp and Vozoff 1977; Christensen, Jacobsen and Sørensen 1990).

It is well established that the joint inversion of galvanic and inductive sounding data will resolve some equivalent parameters appearing in each of the methods and will give a resolution of the subsurface resistivity structure better than either method alone (Raiche *et al.* 1985; Christensen 1989; Sandberg 1993). However, if we attempt a joint inversion of data from galvanic and inductive methods, we must include the coefficient of anisotropy among the model parameters, otherwise we shall encounter inconsistent data sets from the two methods. The inclusion of the coefficient of anisotropy of the layers as a model parameter is not only relevant, it is a necessary condition, introducing about 50% more parameters to be determined from the data.

The earth model, which must be considered when making joint interpretations of galvanic and inductive data sets, is then given by the following parameters: the horizontal resistivity, the coefficient of anisotropy and the thickness of each layer.

Joint interpretation in the presence of macro-anisotropy

We consider a 7-layer model with isotropic layers, given in Table 1. A 10 m-thick top layer of moraine till of resistivity 50 Ωm covers an unsaturated sand and gravel zone of thickness 40 m and resistivity 1000 Ωm. In this zone two low-resistivity clay layers are embedded, each 1 m thick and of resistivity 20 Ωm. Below is a layer of heavy clay of resistivity 5 Ωm. Theoretical data from this model are analysed with 3-layer models, where the second layer is macro-anisotropic.

Table 1 gives the original model, together with the equivalent 3-layer galvanic model,

Table 1. The original 7-layer model, the equivalent galvanic 3-layer model, the equivalent inductive 3-layer model and the equivalent anisotropic 3-layer model.

Layer no.	7-layer model		Galvanic model		Inductive model		Anisotropic model		
	Resistivity (Ωm)	Thickness (m)	Resistivity (Ωm)	Thickness (m)	Resistivity (Ωm)	Thickness (m)	Resistivity (Ωm)	Coefficient of anisotropy, λ	Thickness (m)
1	50	10	50	10	50	10	50	1.00	10
2	1000	12	525	72	290	40	290	1.81	40
3	20	1	5		5		5	1.00	
4	1000	12							
5	20	1							
6	1000	14							
7	5								

the equivalent 3-layer inductive model and the equivalent 3-layer model with an anisotropic second layer. For the second layer we obtain, using (1)–(3),

- $T = 38\,040\,\Omega m^2$, $S = 0.138$ siemens, $H = 40\,m$, $\lambda = 1.81$;
- $\rho_h = 290\,\Omega m$, $\rho_v = 951\,\Omega m$, $\rho_m = 525\,\Omega m$.

We assume that there are 24 geoelectrical sounding data with a density of 10 per decade and $L/2$-distances from $1.58\,m$ to $316\,m$ with a data error of 5%, and 31 transient data with a density of 10 per decade in time from $5\,\mu s$ to $5\,ms$ recorded in a central loop configuration with a $40 \times 40\,m^2$ square loop and an assumed data error of 5%. Both data sets are realistic for DC or TEM soundings. The relative error of the model parameters has been determined as the square root of the diagonal element in the posterior covariance matrix of the least-squares formulation of the inversion problem in the log(data)–log(parameter) space.

In Table 2, a 3-layer interpretation of the galvanic data alone and the transient data alone is shown, together with three joint inversions. The first joint inversion does not include anisotropy. The second joint inversion is for an isotropic 5-layer model. The third joint inversion includes anisotropy, and all coefficients of anisotropy have been left free in the inversion. All forward and inverse modellings were carried out with the SELMA program (Christensen and Auken 1992).

Within the uncertainty of the model parameters, the analysis of the galvanic data alone reproduces the equivalent galvanic model. The resistivity of the third layer is undetermined due to the limited depth penetration caused by the limited range of $L/2$-values for the DC sounding. The analysis of the TEM data alone reproduces the equivalent inductive model, but the thickness of the first layer is poorly determined due to its limited thickness. The resistivity of the second layer is also poorly determined due to its high resistivity. The resistivity of and the depth to the third layer are both very well determined as expected from a TEM sounding. Both interpretations fit the theoretical noise-free data very well with small residuals.

The joint inversion with an isotropic 3-layer model yields a model where depths are determined from the TEM data and resistivities by the DC data. However, there is no sign of the thin clay layers embedded in the high-resistivity second layer. The model parameters appear very well determined as would be expected from a joint inversion, but the fit to the data is poor, considering it is noise-free. The galvanic and inductive data for a 3-layer model are inconsistent. This inconsistency persists in 4-layer models and only the 5-layer model shown in Table 2 fits the data consistently. This 5-layer model allows a conductive zone in the high-resistivity second layer to be detected but not resolved. The parameters of the second and fourth layers are practically undetermined and only the parameters of the first layer and the resistivity of and depth to the third layer are resolved.

The joint inversion taking anisotropy into account reproduces the 3-layer anisotropic model as expected and it fits the data very well. The coefficients of anisotropy are in accordance with the expected values except for the third layer, where the coefficient of anisotropy is undetermined. This is again due to the limited galvanic information about the third layer. Note, however, that the uncertainty in the model parameters has

Table 2. The models resulting from inversion of data from the 7-layer model. The resistivities in the table are the horizontal resistivities.

DC data alone, isotropic model

No.	ρ	SD	Anisotropy	SD	Thickness	SD	Depth	SD
1	49.92	0.02	1.00	0.00	9.54	0.07	9.54	0.07
2	519.50	0.23	1.00	0.00	70.14	0.36	79.67	0.31
3	13.30	2.35	1.00	0.00				
Residual: 0.056								

TEM data alone, isotropic model

No.	ρ	SD	Anisotropy	SD	Thickness	SD	Depth	SD
1	49.50	0.48	1.00	0.00	8.99	1.03	8.99	1.03
2	232.56	0.84	1.00	0.00	41.12	0.25	50.11	0.02
3	5.00	0.03	1.00	0.00				
Residual: 0.001								

Joint inversion, isotropic model

No.	ρ	SD	Anisotropy	SD	Thickness	SD	Depth	SD
1	50.52	0.02	1.00	0.00	11.13	0.03	11.13	0.03
2	995.37	0.03	1.00	0.00	37.65	0.02	48.79	0.01
3	5.14	0.03	1.00	0.00				
Residual: 0.473								

Joint inversion, isotropic model

No.	ρ	SD	Anisotropy	SD	Thickness	SD	Depth	SD
1	50.03	0.02	1.00	0.00	10.08	0.10	10.08	0.10
2	1044.53	1.90	1.00	0.00	14.05	1.91	24.13	1.08
3	40.18	****	1.00	0.00	3.30	****	27.43	1.44
4	1038.12	1.49	1.00	0.00	22.42	1.78	49.85	0.02
5	5.01	0.03	1.00	0.00				
Residual: 0.020								

Joint inversion, anisotropic model

No.	ρ	SD	Anisotropy	SD	Thickness	SD	Depth	SD
1	50.66	0.08	0.98	0.08	9.55	0.09	9.55	0.09
2	250.68	0.18	1.94	0.11	40.46	0.02	50.01	0.01
3	5.01	0.03	0.79	4.41				
Residual: 0.060								

increased compared with the joint isotropic 3-layer inversion: this is because there are three more model parameters to determine.

The above example illustrates that neither galvanic nor inductive data alone will resolve the model in question. It also demonstrates a fundamental dilemma of joint interpretation. If the model is assumed to be isotropic, a joint inversion with 3- and 4-layer models will yield inconsistent data sets, making it preferable to use the 5-layer model, where the conductive zone embedded in the high-resistivity layer is detected. On assuming isotropy the conductive layer is found, which provides support for this approach. However, the layer is not fully characterized and also the parameters of the surrounding layers are poorly determined. Consequently only the presence of the layers is indicated, which in reality is equivalent to a knowledge of the coefficient of anisotropy. Also, with noisy, real data it can be difficult to monitor the inadequacy of the 3- and 4-layer models. The anisotropic 3-layer model clearly identifies an anisotropic second layer and thereby the presence of a conductive zone in the high-resistivity layer.

Determination of electrical anisotropy

In the following the coefficient of anisotropy of the ith layer is indicated by λ_i.

We analyse the possibilities of determining λ_2 in a 3-layer model through joint inversion. The analyses are made with the same assumptions concerning data coverage as in the previous analysis. No *a priori* information has been added so all model parameters are unbound.

In Fig. 2, the six templates display the 441 analyses as grey-scale plots of the relative error of λ_1, λ_2 and λ_3 of a 3-layer model. The 3-layer model has a 10 m-thick top layer of resistivity 50 Ωm, and in this first analysis the resistivity and thickness of the second layer are both varied logarithmically in 10 steps per decade between 0.1 and 10 times the values of the first layer. The third layer has a resistivity of 5 Ωm. The thickness of the second layer varies along the horizontal axis of the templates, and the resistivity of the second layer varies along the vertical axis. Thus in the top half of the templates we find the maximum models, while in the bottom half we have the double decreasing models. The left side of the templates represents small thicknesses and the right side large thicknesses.

In Fig. 2 we first analyse how λ_1, λ_2 and λ_3 are determined as a function of the resistivity and thickness of the second layer. This analysis is carried out for two different values of λ_2. In the top row $\lambda_2 = 1.8$, while in the bottom row $\lambda_2 = 1.2$. In both cases $\lambda_1 = \lambda_3 = 1$. It should be noted that the two rows are very similar, which means that the determination of the coefficients of anisotropy is not very dependent on λ_2.

From Fig. 2 we see that λ_1 is generally well determined. λ_2 is better determined as the second layer gets thicker and the determination becomes poorer as the resistivity of the second layer gets larger. An increase in the resistivity of the second layer means that the determination from the TEM data of the horizontal resistivity becomes poorer and the contribution of the galvanic data to the determination of the thickness decreases. λ_3
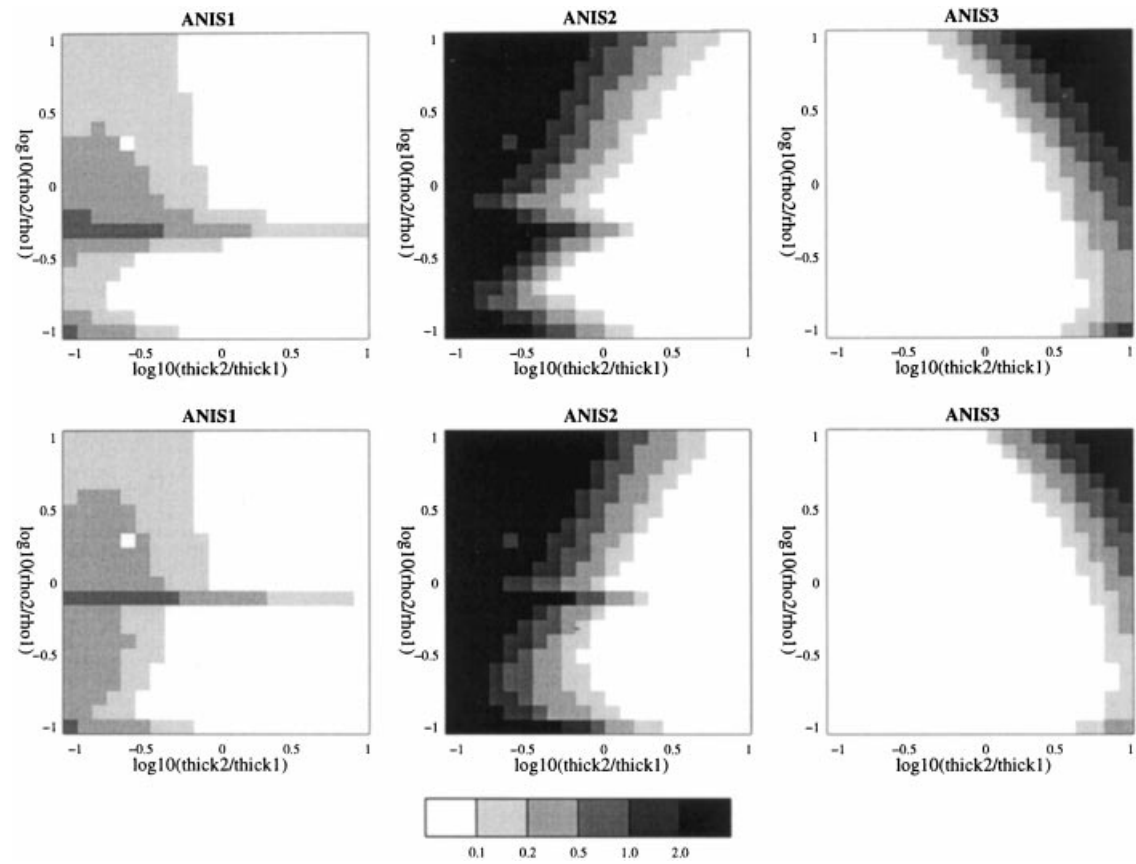
Figure 2. The relative error in the determination of the coefficients of anisotropy for a 3-layer model as a function of the thickness and resistivity of the second layer. $\lambda_1 = \lambda_3 = 1$. In the top row $\lambda_2 = 1.8$ and in the bottom row $\lambda_2 = 1.2$.

is generally well determined but the determination deteriorates for large thicknesses and resistivities of the second layer, which would be expected as the galvanic information about the third layer decreases with increasing thickness and resistivity of the second layer. A zone of higher error extends from the left side of the templates concerning the first and second layers. For the top row this corresponds to a value of ρ_2 equal to $0.5 \times \rho_1$. For this value the DC resistivity of the second layer is $0.5 \times \rho_1 \times 1.8 \approx \rho_1$, so the DC resistivity contrast between the first and the second layer is very small. For the bottom row this feature is seen for a value of ρ_2 of $0.8 \times \rho_1$. Again we see that for this value, the DC resistivity of the second layer is $0.8 \times \rho_1 \times 1.2 \approx \rho_1$.

In the next analyses we see how λ_2 is determined for a high-resistivity second layer as a function of the thickness and the coefficient of anisotropy of the second layer. The resistivity of the second layer has been set at $300\,\Omega$m. In the templates of Fig. 3, λ_2 now varies linearly on the *Y*-axis. In the top row, no *a priori* information has been included. In the bottom row, λ_1 and λ_3 have been given the *a priori* value of 1 with a relative uncertainty of 0.001, i.e. the first and third layer are assumed to be isotropic.

The left templates of Fig. 3 show what was already indicated in Fig. 2: that the determination of λ_2 does not depend heavily on its value. It is seen that λ_2 is better determined the thicker the second layer, and it is not well determined unless the thickness of the second layer is greater than 3–4 times the thickness of the first layer.

However, more informative than the relative error in λ_2, $\Delta\lambda_2/\lambda_2$, is the error relative to the difference between λ_2 and unity, $\Delta\lambda_2/(\lambda_2 - 1)$, since $(\lambda_2 - 1)$ determines the deviation from an isotropic layer. The right templates of Fig. 3 show this relative error, $\Delta\lambda_2/(\lambda_2 - 1)$. If the relative error of the deviation is considered, one more requirement is added: that the thickness of the second layer should be large compared with the top layer, i.e. that λ_2 should not be too small. λ_2 is not well determined unless it is greater than 1.5. According to (5) this corresponds to a minimum resistivity contrast of 6.85.

Comparing the top and bottom rows of Fig. 3, we see that the inclusion of *a priori* information about the isotropy of the top and bottom layers improves the determination of λ_2 slightly, but the main conclusions remain unchanged.

Anisotropy of realistic earth models

The above analysis which shows the principal possibilities and limitations in the determination of anisotropy was carried out for simple 3-layer models. In this section we see how anisotropy can be determined in a realistic 1D earth model constructed from an electrical log recorded with the Ellog method.

The Ellog method is an auger-drilling method, by which an electrical log (and a gamma log) are measured continuously while actively drilling, using tools integrated in the hollow drilling stem (Sørensen 1994). Because drilling mud is not used, no invasion zone exists, and the measured resistivity of the formation provides a very good estimate of the true formation resistivity. With the Ellog, it is also possible to measure the formation resistivity of the unsaturated zone. The resistivity is measured with a vertical Wenner configuration with an electrode spacing of 0.2 m. The electrodes are mounted
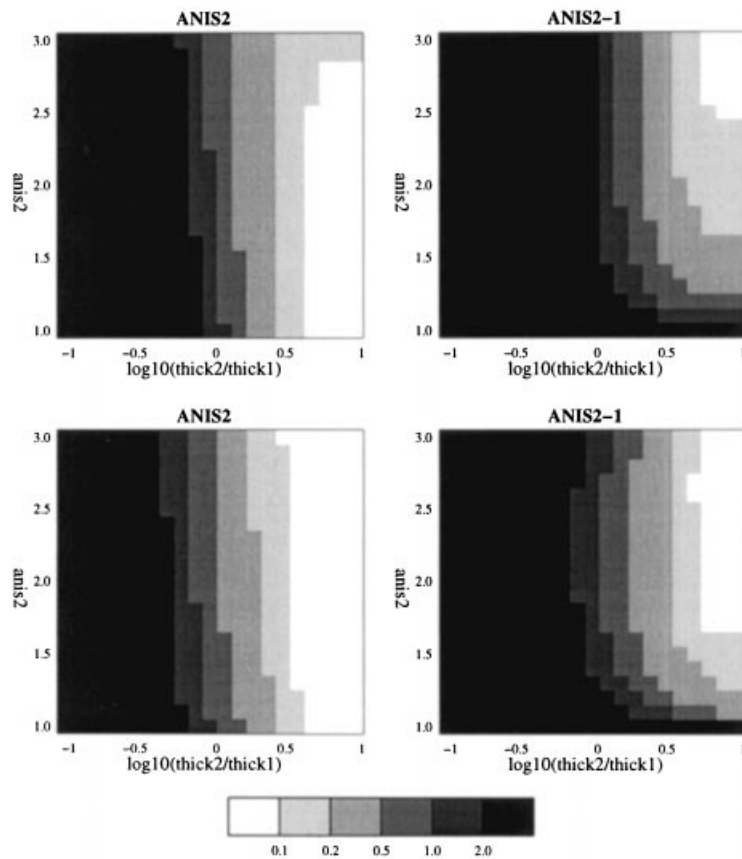
Figure 3. The relative error in λ_2 of a 3-layer model as a function of the thickness and coefficient of anisotropy of the second layer. $\lambda_1 = \lambda_3 = 1$. The left column relates to λ_2, the right column to $(\lambda_2 - 1)$. The resistivity of the second layer is set at 300 Ωm. In the top row no *a priori* information has been added. In the bottom row λ_1 and λ_3 have been fixed at 1 with uncertainty 0.001, i.e. the first and third layers are assumed to be isotropic.

in insulating material about 1 m from the cutting head of the stem (Sørensen 1989). Measurements are taken every 2–4 mm, each measurement being an average of 80 samples, resulting in an extremely detailed log with a high vertical resolution. As the drilling is performed with an auger–drill stem with a cutting head and a flight to transport the loose material to the surface, there is minimal pressure on the formation and thereby minimal perturbation of the resistivity of the formation. The flight of the auger is only 16 mm high and tank experiments have shown that the material transported by the flight, though it may be different from the material further out in the formation, will have a negligible effect on the measured resistivity (Sørensen 1989). The method has been used extensively in hydrogeophysical investigations since 1989 and more than 25 000 m have been drilled.
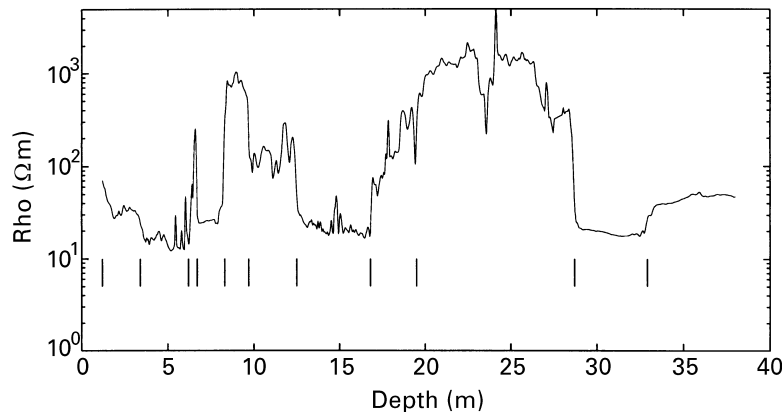
Figure 4. The electrical log, Rokballe 03, recorded with the Ellog method. The vertical lines indicate the layering used in the analysis and calculation of the model responses.

The electrical log, Rokballe 03, shown in Fig. 4, belongs to a series of Ellogs made in connection with a hydrogeophysical investigation in the Rokballe area, 15 km south of Aarhus. In the area a large exploitation of groundwater has resulted in a lowering of the groundwater table by 10–15 m over the last two decades. The top part of the log down to a depth of 8.3 m displays fairly low resistivities corresponding to clays and clayey till with a thin sand layer between 6.2 m and 6.7 m. Between 8.3 m and 12.5 m there is a sandy formation where the bottom part is saturated. At 9.7 m there is a perched water table. From 12.5 m to 16.8 m we find clay and below 16.8 m we find predominantly sand and gravel, unsaturated down to 28.7 m and saturated below this level. At 23.5 m we find a thin clay layer. The lower resistivity between 32.9 m and 38.1 m is caused by the high sulphate content of the groundwater created by the oxidation of pyrite from the newly created unsaturated zone between 19.5 m and 28.7 m. The log has been selected because it is typical of the Quaternary geology in large areas of Denmark.

If we assume that the resistivity varies linearly in a semilogarithmic plot between the measuring points, the resistivity between neighbouring measuring points, z_a and z_b, can be written as

$$\rho(z) = \rho_a \cdot \exp\left[\ln(\rho_b/\rho_a)\frac{z - z_a}{z - z_b}\right], \quad z_a \leq z \leq z_b,$$

where ρ_a and ρ_b are the measured resistivities at z_a and z_b, respectively. The effective transverse resistance $T(z_a, z_b)$ and the effective horizontal conductance $S(z_a, z_b)$ of the interval can be found from

$$T(z_a, z_b) = \int_{z_a}^{z_b} \rho(z)\mathrm{d}z = \frac{(\rho_b - \rho_a)(z_b - z_a)}{\ln(\rho_b/\rho_a)},$$

$$S(z_a, z_b) = \int_{z_a}^{z_b} \rho(z)^{-1}\mathrm{d}z = \frac{1}{\rho_a\rho_b}\frac{(\rho_b - \rho_a)(z_b - z_a)}{\ln(\rho_b/\rho_a)}.$$

Summing the effective resistances and conductances between two adjacent measurements, the total resistance and the total conductance for a specific depth interval can be found from (3) and the vertical and horizontal resistivities and the coefficient of anisotropy can be found from (2). The log in Fig. 4 has been divided into 11 layers indicated by the vertical lines, and for each layer the horizontal resistivity and the coefficient of anisotropy has been calculated. The model has been supplemented with a good conductor of 5 Ωm at 80 m depth, which is known to be present in the area (indicated with a dotted line in Fig. 4). Using this anisotropic 12-layer model, theoretical data have been calculated for a DC sounding and a TEM sounding. There are 23 geoelectrical sounding data with a density of 10 per decade and with $L/2$-distances from 1.58 m to 251 m. There are 26 transient data with a density of 10 per decade in time from 6.3 µs to 2 ms recorded in a central loop configuration with a $40 \times 40 \, \text{m}^2$ square loop. The assumed data error is 5% in all data. The data sets have been inverted individually and jointly for the earth model with the minimum number of layers that would fit the data. Figure 5 and Table 3 show the results of the inversions.

The first feature to be observed is that data from soundings over the rather complicated model revealed by the electrical log can be interpreted with very few layers. This confirms the well-known poor resolution capability of surface electrical and electromagnetic methods.

A separate inversion of the DC data can be carried out with a 4-layer model. The 4-layer model recognizes the two clay layers indicated in the top of the log but treats the high-resistivity layers and the clay layer as one separate layer. The depth to the good conductor is incorrectly determined and not resolved.

The separate inversion of the transient data can be carried out with a 3-layer model. The model interprets the top clay formation as one layer, while the whole sequence of high-resistivity layers and the sand below the water table are treated as one layer. The depth to and the resistivity of the good conductor is of course correctly found and very well determined.

A joint inversion with anisotropic layers can be carried out with a 5-layer model. A 4-layer model is also able to satisfy the data sets, but the model parameters obtained are completely distorted, with very high and very low values of the coefficient of anisotropy. The 5-layer model distinguishes the two top layers in the same way as the separate DC inversion, but the high-resistivity layer with its embedded clay layer and part of the saturated sand formation are all combined into one anisotropic sequence. The resistivity of the fourth layer is too low compared with the true model. The depth to the good conductor and its resistivity are well determined.

A joint inversion with an isotropic model has also been tried. In this case, a 7-layer model must be used, as the 5- and 6-layer models are insufficient to fit the data. Essentially the 7-layer model reproduces the main features of the model with the two clayey top layers, the high-resistivity layers separated by the clay layer, and the sixth layer (the saturated sand) having the right resistivity. The depth to and the resistivity of the good conductor are also well determined.

This example with a complicated model illustrates some of the intricacies of joint
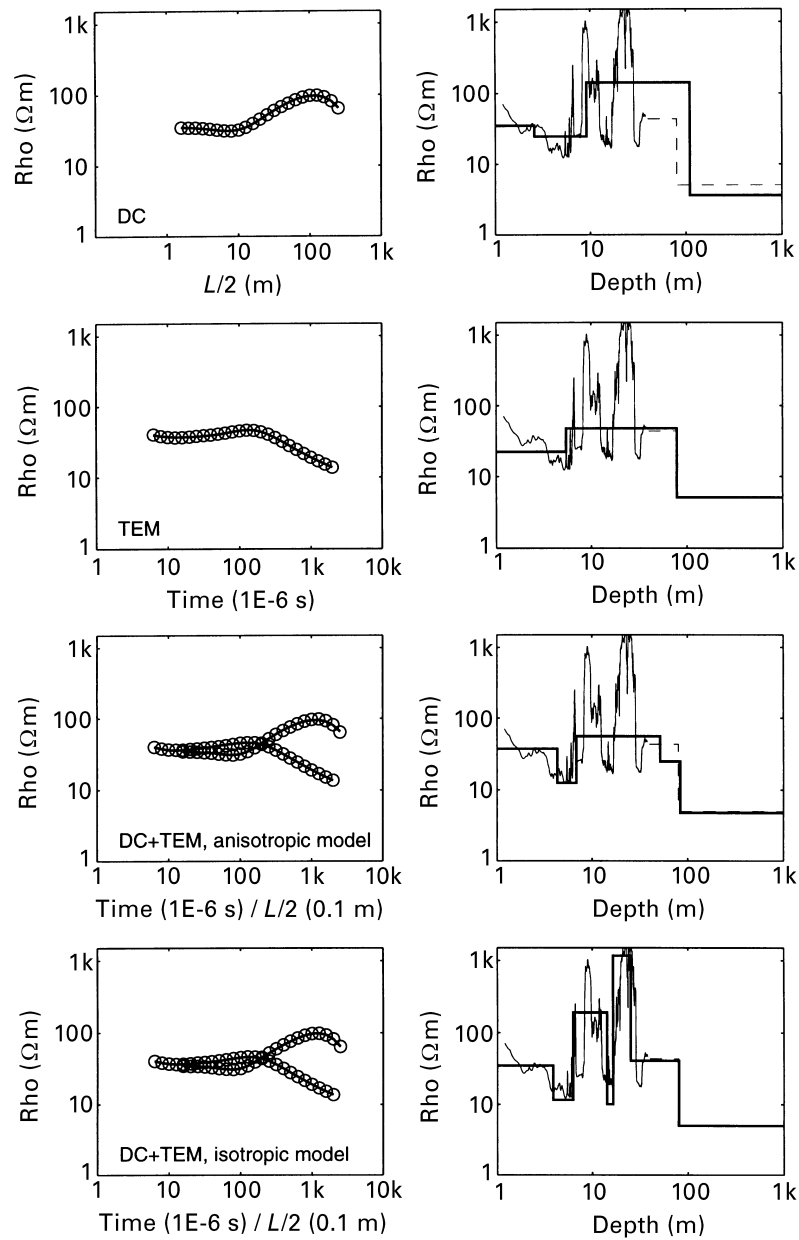
Figure 5. The results of individual and joint inversions of the data calculated from the model based on the electrical log of Fig. 4. The left column shows the data and model response, the right column shows the model together with the electrical log. Note that the models and the electric log in the right column frames are plotted on a logarithmic scale.

Table 3. The models resulting from inversion of data created from the electrical log of Fig. 4. The resistivities in the table are the horizontal resistivities.

DC data alone, isotropic model

No.	ρ	SD	Anisotropy	SD	Thickness	SD	Depth	SD
1	35.11	0.04	1.00	0.00	2.59	0.62	2.59	0.62
2	24.62	0.29	1.00	0.00	6.56	0.56	9.15	0.24
3	141.37	0.15	1.00	0.00	100.90	0.54	110.04	0.48
4	3.56	****	1.00	0.00				

Residual: 0.157

TEM data alone, isotropic model

No.	ρ	SD	Anisotropy	SD	Thickness	SD	Depth	SD
1	22.27	0.38	1.00	0.00	5.43	0.89	5.43	0.89
2	47.34	0.06	1.00	0.00	73.50	0.08	78.93	0.03
3	5.12	0.09	1.00	0.00				

Residual: 0.128

Joint inversion, anisotropic model

No.	ρ	SD	Anisotropy	SD	Thickness	SD	Depth	SD
1	37.62	0.18	0.92	0.18	4.30	0.33	4.30	0.33
2	12.53	0.79	1.00	0.20	2.53	0.90	6.83	0.16
3	56.26	0.07	2.33	0.06	44.75	0.17	51.58	0.14
4	24.85	0.39	1.01	0.20	32.09	0.19	83.67	0.05
5	4.79	0.13	1.00	0.20				

Residual: 0.624

Joint inversion, isotropic model

No.	ρ	SD	Anisotropy	SD	Thickness	SD	Depth	SD
1	34.83	0.03	1.00	0.00	3.87	0.82	3.87	0.82
2	11.52	6.02	1.00	0.00	2.39	7.70	6.26	2.45
3	188.63	8.89	1.00	0.00	7.98	****	14.24	4.97
4	10.06	****	1.00	0.00	2.25	****	16.48	2.88
5	1166.37	6.37	1.00	0.00	8.69	6.41	25.17	0.39
6	40.72	0.27	1.00	0.00	55.25	0.14	80.42	0.04
7	4.97	0.11	1.00	0.00				

Residual: 0.023

inversion in general and the determination of electrical anisotropy in particular. First of all it must be stressed that the data used are consistent 1D data calculated from a 1D model, so inconsistencies between the galvanic and inductive data sets cannot be responsible for the difficulties encountered. A comparison of the results obtained using an anisotropic and an isotropic model in the inversion suggests that the 7-layer isotropic model is a better reflection of the true model. This presupposes that the true model is known, and that is not the case in real life. In reality there is no more information in the 7-layer isotropic model than in the 5-layer anisotropic model because the third, fourth and fifth layers are completely undetermined as seen from Table 3. All that can be said is that both high and low resistivities are present in this depth range, but that is equivalent to the results obtained with the 5-layer anisotropic model. However, the finding of an incorrect resistivity for the fourth layer of the anisotropic 5-layer model is not understood, but it probably reflects the complexity of the joint inversion of data from a complex model.

It is instructive to compare the resistivities and coefficients of anisotropy obtained from the inversions with the values obtained from the log, the 'true' model, by averaging over the layers of the inversions. In Table 4, this is carried out for the 5-layer anisotropic model and the 7-layer isotropic model. It is seen that the anisotropic model does determine a coefficient of anisotropy of the third layer in accordance with the log. In general there is the same amount of discrepancy between the model and the log for the 5-layer and the 7-layer models.

Discussion and conclusion

As stated in the previous sections, it would be desirable to be able to find the coefficient of anisotropy from joint inversion. A reliable estimate of the coefficient of anisotropy would be a valuable indicator that the combined model elements of the interpretation were composed of layers of different resistivities. In hydrogeological investigations this may indicate the presence of layers that could severely influence the flow of groundwater, and in the mapping of raw materials the coefficient of anisotropy could be used as an indicator of quality.

The application of galvanic soundings or inductive soundings alone does not allow the coefficient of anisotropy to be resolved, but the joint use of galvanic and inductive methods can do so. Also, the anisotropy of the model layers must be taken into account in joint 1D interpretations of electrical and electromagnetic soundings.

Analyses show that an anisotropic layer has to be thick relative to the thickness of the overburden before its coefficient of anisotropy can be determined. Also, the coefficient of anisotropy must not be too small if a layer is to be reliably categorized as anisotropic. This latter result implies that it is much more difficult to determine anisotropy in the saturated zone, where resistivity contrasts are small and thus the coefficient of anisotropy is smaller than in the unsaturated zone. Hence, for complicated earth models – and real geology is not simple – there are reasons both for and against using anisotropic models.

Table 4. Comparison of the model parameters obtained by joint inversion with the values obtained from the log averaging over the layers of the inversions for the anisotropic 5-layer model and the isotropic 7-layer model.

Parameter/Model	ANIS-5	LOG-5	ISO-7	LOG-7
ρ_1	37.62	28.21	34.83	30.78
ρ_2	12.53	18.56	11.52	15.88
ρ_3	56.26	46.87	188.63	49.22
ρ_4	24.85	23.14	10.06	21.12
ρ_5	4.79	5.00	1166.37	189.03
ρ_6	–	–	40.72	39.75
ρ_7	–	–	4.97	5.00
λ_1	0.92	1.06	1.00	1.04
λ_2	1.00	1.32	1.00	1.03
λ_3	2.33	2.46	1.00	1.99
λ_4	1.01	1.30	1.00	1.03
λ_5	1.00	1.00	1.00	2.14
λ_6	–	–	1.00	1.48
λ_7	–	–	1.00	1.00

Finally, since the coefficient of anisotropy is often a poorly determined model parameter, inconsistencies between the galvanic and inductive data sets, for example from noise or deviations from a 1D model structure, will often distort the coefficient of anisotropy to make the model fit the data in a joint inversion.

Although the general presence of macro-anisotropy must be recognized, it seems that there are severe limitations in our ability to determine quantitatively the coefficient of anisotropy.

References

Campbell D.L. 1977. Model for estimating electric macroanisotropy coefficient of aquifers with horizontal and vertical fractures (short note). *Geophysics* **42**, 114–117.

Chlamtac M. and Abramovici F. 1981. The electromagnetic fields of a horizontal dipole over a vertically inhomogeneous and anisotropic earth. *Geophysics* **46**, 904–915.

Christensen N.B. 1989. AC resistivity sounding. *First Break* **7**, 447–452.

Christensen N.B. 1992. On the importance of determining electrical anisotropy in hydro-geological investigations. 54th EAEG meeting, Paris, France, Extended Abstracts, 712–713.

Christensen N.B. and Auken E. 1992. Simultaneous electromagnetic layered model analysis. In: *Proceedings of the Interdisciplinary Inversion Workshop 1, Aarhus* (ed. B.H. Jacobsen). *GeoSkrifter* **41**, 49–56.

Christensen N.B., Jacobsen B.H. and Sørensen K.I. 1990. The determination of electrical anisotropy and its hydrogeological significance. 52nd EAEG meeting, Copenhagen, Denmark, Extended Abstracts, 122.

Jupp D.L.B. and Vozoff K. 1977. Resolving anisotropy in layered media by joint inversion. *Geophysical Prospecting* **25**, 460–470.

Keller G.V. and Frischknecht F.C. 1966. *Electrical Methods in Geophysical Prospecting*. Pergamon Press, Inc.

Raiche A.P., Jupp L.B., Rutters H. and Vozoff K. 1985. The joint use of coincident loop transient electromagnetic and Schlumberger sounding to resolve layered structures. *Geophysics* **50**, 1618–1627.

Sandberg S.K. 1993. Examples of resolution improvement in geoelectrical soundings applied to groundwater investigations. *Geophysical Prospecting* **41**, 207–227.

Sinha A.K. and Bhattacharya P.K. 1967. Electrical dipole over an anisotropic and inhomogeneous Earth. *Geophysics* **32**, 652–667.

Sørensen K.I. 1989. A method for measurement of the electrical formation resistivity while auger drilling. *First Break* **7**, 403–407.

Sørensen K.I. 1994. The Ellog auger drilling method. *Proceedings of the Symposium on the Application of Geophysics to Engineering and Environmental Problems, Boston, Massachusetts, USA*, pp. 985–994.

Ward S.H. and Hohmann G.W. 1989. Electromagnetic theory for geophysical applications. In: *Electromagnetic Methods in Applied Geophysics. Investigations in Geophysics*, Vol. 3 (ed. M.N. Nabighian), pp. 131–311. SEG, Tulsa, OK.